On stabilisation of compositional density jumps in compressible mantle convection simulations

Paul James Tackley1

¹Department of Earth and Planetary Sciences, ETH Zurich, Zurich, 8092, Switzerland

5 Correspondence to: Paul J. Tackley (ptackley@ethz.ch)

Abstract. Large density jumps in numerical simulations of solid Earth dynamics can cause numerical "drunken sailor" oscillations. An implicit method has previously been shown to be very effective in stabilising the density jump that occurs at a free surface against such instabilities (Kaus et al., 2010; Duretz et al., 2011). Here the use of this to prevent oscillations of compositional layers deeper in the mantle is examined. If the stabilisation algorithm uses the total density field including the steady increase of density with depth due to adiabatic compression and jumps due to phase transitions then a severe artificial reduction of convective vigour occurs because the algorithm assumes that density is advected with the flow but these density gradients are not. This artificial vigour reduction increases with Rayleigh number but decreases with decreasing grid spacing. Thus, it is essential to use only composition-related density gradients in the stabilisation algorithm, and a simple method for isolating these is presented. Once this is done, the stabilisation method works effectively for internal compositional layers as well as a free surface.

1. Introduction

Density jumps due to treatment of a free surface by the "sticky air" method (e.g. Crameri et al., 2012), in which the surface is represented as an abrupt interface between rock and low-density, low-viscosity "air", can induce numerical "drunken sailor" instabilities, in which the free surface oscillates up and down on successive time-steps, overshooting its equilibrium position.

To cure this problem, an implicit free-surface stabilisation algorithm was introduced, initially for the finite-element discretization (Kaus et al., 2010; Andrés-Martínez et al., 2015) and then for the staggered-grid finite difference (equivalent to finite-volume) discretization (Duretz et al., 2011). The basis of this scheme is that when calculating the flow field, the change in buoyancy due to advection of density during a time step is treated implicitly; while this is applied throughout the domain, by far the largest correction comes from advection of the free surface. It is very effective in stabilising the free surface, allowing a normal (e.g. Courant condition limited) time-step to be used (Kaus et al., 2010; Duretz et al., 2011). A subsequent rigorous stability analysis led to an alternative approach using an explicit scheme based on nonstandard finite differences (Rose et al., 2017). Fully implicit time stepping in the entire domain is another alternative (Popov and Sobolev, 2008; Kramer et al., 2012).

In global mantle convection simulations, compositional density jumps can also arise inside in the mantle, typically due to a primordial layer of dense material above the core-mantle boundary (CMB) (e.g. Gurnis, 1986; Tackley, 1998; Davaille,

Deleted: J.

Deleted: motion

Deleted: the free surface

(Deleted:

where Δt is the time step. These density changes can be treated implicitly by substituting ρ_{new} for ρ in (1) and moving the velocity term to the left-hand side:

65
$$-\nabla p + \nabla \cdot \underline{\tau} - \theta \Delta t (\vec{v} \cdot \nabla \rho) \vec{g} = -\rho \vec{g}$$
 (4)

where θ is a factor between 0 (explicit) and 1 (implicit). The finite-difference stencil for velocity components is modified accordingly, based on $\nabla \rho$ calculated at the beginning of the time step. In practice, in the vicinity of a near-horizontal layer interface it is vertical motions that change the density so a simplified version considering only vertical (z) velocities and assuming that g is vertical has almost the same stabilisation effect:

70
$$-\nabla p + \nabla \cdot \underline{\underline{\tau}} - \theta \Delta t \left(v_z \frac{\partial \rho}{\partial z} \right) g \hat{\overline{z}} = -\rho g \hat{\overline{z}}$$
 (5)

2.2 Continuity equation

The full continuity (conservation of mass) equation can be written in Eulerian form as

$$\nabla \cdot (\rho \vec{v}) = -\frac{\partial \rho}{\partial t} \tag{6}$$

or Lagrangian form as

75
$$\rho \nabla \cdot \vec{v} = -\frac{D\rho}{Dt}$$
 (7)

These equations are commonly approximated bearing in mind that thermally induced density differences are of order 1%, which is much smaller than density differences due to adiabatic compression + phase transitions over the depth of the mantle (~65%) or due to compositional differences such as a free surface (discussed above) or iron diapirs (e.g. Samuel and Tackley, 2008; Lin et al., 2011) (~100%). Furthermore, for whole-mantle studies dynamic (i.e. related to the flow) pressure is much smaller than hydrostatic pressure, so its effect on density is typically ignored. Thus, (7) is often approximated as

$$\nabla \cdot \vec{v} = 0$$

This is valid when density is advected with the flow, but invalid when there are significant non-advected density variations such as due to pressure or phase transitions. In this study it is necessary to model flow with both large pressure-related density variations and large composition-related density variations so a modified form of (7) is considered, decomposing the Lagrangian density time-derivative into temperature (T)-, pressure (P)- and composition (C)-related components:

$$\rho \nabla \cdot \vec{v} = -\frac{D\rho}{Dt} = -\left(\frac{D\rho}{Dt}\right)_T - \left(\frac{D\rho}{Dt}\right)_P - \left(\frac{D\rho}{Dt}\right)_C \tag{9}$$

T-induced variations are assumed to be negligible, consistent with the Boussinesq or compressible anelastic approximations (additionally, T changes slowly in the Lagrangian frame). The compositional component is zero in the Lagrangian frame and,

Deleted: Where

90 ignoring dynamic pressure as in the Boussinesq or anelastic approximation, the pressure component is due only to vertical motion as:

$$\rho \nabla \cdot \vec{v} = -\left(\frac{D\rho}{Dt}\right)_{D} = -v_{z} \frac{\partial \rho}{\partial z} \tag{10}$$

This can be satisfied using a z-dependent density that increases due only to hydrostatic compression:

$$\nabla \cdot (\rho_{-}\vec{v}) = 0 \tag{11}$$

where ρ_z is a depth-dependent reference density that depends only on hydrostatic compression, not composition. It would be possible to implement a more accurate version of the continuity equation that includes temperature and dynamic pressure effects (e.g. Gassmöller et al., 2020) but the current level of approximation suffices for the tests presented and is consistent with the commonly-used anelastic approximation (King et al. 2010).

2.3 Energy equation

100 For the tests performed here a simple form of energy conservation is assumed:

$$\rho C_p \frac{\partial T}{\partial t} = k \nabla^2 T - \rho C_p \vec{v} \cdot \nabla T \tag{12}$$

where T is temperature, t is time, C_ρ is specific heat capacity, and k is thermal conductivity. Normally, when taking compressibility into account, terms for adiabatic heating/cooling and viscous dissipation would appear in this equation. This version corresponds to the limit of zero Grüneisen parameter ($\gamma = \partial \ln T / \partial \ln \rho$), or in nondimensional terms, having a zero dissipation-number but finite compressibility-number (Tackley, 1996). The concept is to make the test program as simple as possible to demonstrate what is discussed in this manuscript.

2.4 Test program

The associated test program CConv2dDJS.jl posted on Zenodo (Tackley and ETH Zurich, 2025) is written in the Julia programming language (Bezanson et al., 2017) and solves a nondimensional version of the equations above in two dimensions, x (horizontal) and z (vertical). The continuity equation is identical to equation (11) above, with ρ_z being 1.0 at the surface and increasing linearly to a specified value at the CMB. The two components of the momentum equation are:

$$-\frac{\partial p}{\partial x} + \frac{\partial \tau_{xx}}{\partial x} + \frac{\partial \tau_{xz}}{\partial z} = 0 \qquad -\frac{\partial p}{\partial z} + \frac{\partial \tau_{zz}}{\partial z} + \frac{\partial \tau_{zx}}{\partial x} - v_z \Delta t \frac{\partial \rho}{\partial z} B_{air} Ra = -Ra \left(T - B_{air} C_{air} - B_{DL} C_{DL} \right)$$
(13)

where Ra is the Rayleigh number, $C_{\rm air}$ and $C_{\rm DL}$ are the fraction (0-1) of air and dense layer, respectively, and $B_{\rm air}$ and $B_{\rm DL}$ are the compositional buoyancy ratios for air and dense layer, respectively ($B_\chi = \Delta \rho_\chi/(\rho \alpha \Delta T)$) where α is thermal

expansivity and ΔT is the temperature drop across the layer). $\underline{\theta}$ in equation (5) is assumed to be 1.0. For air, the buoyancy

Deleted: Θ

parameter is negative (air being less dense than rock) and has a value $B_{air} = -1/(\alpha\Delta T) \approx -1/(2.10^{-5} \times 2500) = -20$ whereas B_{DL} is positive and has a much smaller magnitude. The mechanical boundary conditions are impermeable and free slip (zero shear stress) on all boundaries.

20 The nondimensional energy equation is:

$$\rho_{tot} \frac{\partial T}{\partial t} = \nabla^2 T - \vec{v} \cdot \nabla T \tag{14}$$

Thermal boundary conditions are insulating side boundaries and isothermal top and bottom boundaries (T=0 and 1, respectively). The equivalent equation for composition lacks the diffusion term.

Density is the sum of pressure-related, composition-related and phase transition-related components:

125
$$\rho_{tot} = \rho_z + \Delta \rho_C + \Delta \rho_{pT} \tag{15}$$

Where ρ_z is 1.0 at the surface and increases linearly to a specified value at the CMB, the compositional component is given by

$$\Delta \rho_C = C_{nir} \Delta \rho_{nir} + C_{DI} \Delta \rho_{DI} = -C_{nir} - C_{DI} B_{DI} / B_{nir}$$

$$\tag{16}$$

(noting that $\Delta \rho_{air} = -1$ nondimensional and $\Delta \rho_{DL} = \Delta \rho_{air} B_{DL} / B_{air} = -B_{DL} / B_{air}$), and $\Delta \rho_{PT}$ is zero above the phase

transition depth and the specified density increase below the phase transition depth, corresponding to a sharp phase transition with zero Clapeyron slope.

The continuity equation uses ρ_z as explained above, while the energy equation uses ρ_{tot} . The DJS algorithm can either correctly use $\Delta\rho_C$ or incorrectly use ρ_{tot} in order to illustrate the bad artefacts that result.

The equations are discretized using a standard staggered-grid finite volume discretization (e.g. Harlow and Welch 1965; Patankar, 1980), as used by many codes in the geodynamical modelling community (e.g. Ogawa et al., 1991; Tackley, 1993; Trompert and Hansen, 1996; Gerya and Yuen, 2007; Kameyama et al. 2008; Tackley, 2008; Kaus et al., 2016). The velocity-pressure solution is solved with a direct solver utilising the built-in "\" operator. Advection of temperature and composition is performed using an upwind donor-cell technique, which is very diffusive but suffices for the tests here. Temperature diffusion is calculated using explicit finite differences.

3. Results

3.1 Surface or dense layer stabilisation

First, it is verified that the implementation of the DJS algorithm in the attached program eliminates "drunken sailor" oscillations. Figure 1 shows the effectiveness of the algorithm for preventing oscillations of a free surface with a sticky air layer. Detailed tests are not performed here because they have been already been reported elsewhere (Duretz et al., 2011). Figure 2 shows the effectiveness of the algorithm for stabilising a dense layer above the CMB. In both cases, oscillations occur

Formatted: English (US)

Deleted: $\Delta \rho_C = -C_{air} + C_{DL}B_{DL} / B_{air} \rightarrow \rightarrow$

Deleted: and $\Delta
ho_{\scriptscriptstyle PT}$

Deleted: ρ_{tot}

Deleted: $\Delta \rho_c$

Deleted: $ho_{\scriptscriptstyle tot}$

150 with the algorithm switched off, but a smooth evolution is obtained with the algorithm switched on. When oscillations occur, the compositional interface (free surface or top of layer) becomes smeared out due to the numerical diffusion inherent in the upwind donor cell advection algorithm. In contrast, when the interface barely moves there is negligible numerical diffusion so the interface remains fairly sharp.

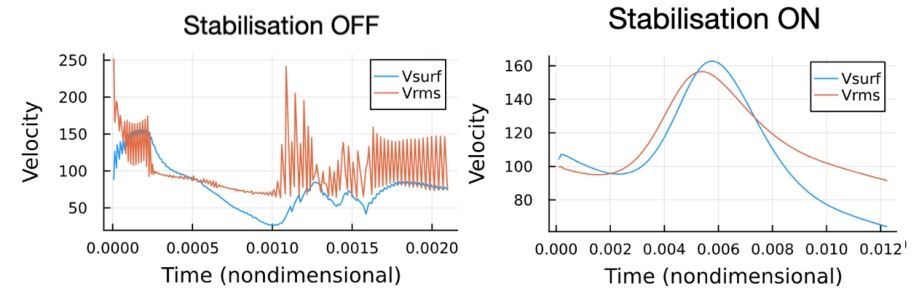


Figure 1. Stabilisation of a sticky-air layer with viscosity contrast 0.001 and thickness 0.2 on a 32x32 grid with Ra=10⁵.
Oscillations occur when density jump stabilisation is switched off (left) but not when it is switched on (right).

3.2 Convection with depth-dependent density

Steady-state convection solutions are calculated for various density increases with depth (ρ_{cmb}/ρ_{surf}), various Rayleigh numbers from 10^4 to $3x10^5$, and two grid resolutions (32x32 and 64x64). The calculations are run until the top and bottom Nusselt numbers are identical and the rms velocity has stopped changing, which typically requires 1000s of time steps. These tests do not have any compositional density variations so the DJS algorithm is not needed; their purpose is to demonstrate the problems that occur when it is applied to non-compositional density variations.

The influence of compressibility is tested first, varying the density increase with depth (ρ_{cmb}/ρ_{surf}) from factor 1.0 to 2.0, bearing in mind that in Earth this ratio is about 1.65 (including compressibility and phase transitions). Correct solutions (using only non-existent composition-dependent density gradients in the DJS algorithm) are compared to those using the full density field (Figure 3 left column). Solutions indicate that the correct Nusselt number (top left) and V_{rms} (middle left) change slightly with ρ_{cmb}/ρ_{surf} , slightly increasing and decreasing, respectively. Resolution makes little difference to the correct values. With DJS using the full density field, however, Nusselt number and V_{rms} decrease substantially as ρ_{cmb}/ρ_{surf} is increased. Ratios are plotted in the lower left. In the worst case (ρ_{cmb}/ρ_{surf} =2.0, 32x32 grid), Nusselt number is decreased by 35% and V_{rms} by about 65%. This magnitude of reduction depends on grid resolution: with a 64x64 grid the effect is about half as much as with a 32x32 grid. This is because the effect is proportional to the time step, which is about a factor of two smaller with the 64x64 grid.

Deleted: the

Deleted: DGS

If one wishes to include horizontal density gradients in the DJS algorithm as in equation (4), the procedure is the same as that above (equations 17-20) for each horizontal direction.

40 4.2 Conclusions

The density-jump stabilisation algorithm of (Duretz et al., 2011) is an effective method of preventing numerical oscillations of internal compositional layers as well as of a free surface. However, it is essential that the density gradient used in the algorithm is that for compositional density variations only, otherwise severe artefacts result. If the used density gradient incorrectly includes the steady density increase with depth due to adiabatic compression and/or density jumps due to phase transitions, a severe reduction of convective vigour results. This reduction increases with Rayleigh number but decreases with increasing numerical resolution. Isolating the compositional component of the density gradient can be straightforwardly done using the approach presented in this paper.

Code availability. The exact version of the Julia code used to produce the results and figures in this paper is archived on Zenodo under the MIT license under DOI 10.5281/zenodo.15115817 (Tackley and ETH Zurich, 2025). No input data or additional scripts are required. The Julia script used to produce the graphs in Fig. 3 is also archived there.

Competing interests. The author declares that he has no conflict of interest.

Special issue statement. Advances in numerical modelling of geological processes.

Acknowledgments. Identifying and fixing these problems at this point in time was motivated by dense layer oscillations identified by Elena Zaharia and Maxim Ballmer. <u>Helpful reviews were provided by Mingming Li and Boris Kaus.</u>

255 References

Andrés-Martínez, M., Morgan, J. P., Pérez-Gussinyé, M. and Rüpke, L.: A new free-surface stabilization algorithm for geodynamical modelling: Theory and numerical tests, Phys. Earth Planet. Int., 246, 41-51, doi:10.1016/j.pepi.2015.07.003, 2015

Bezanson, J., Edelman, A., Karpinski, S. and Shah, V. B: Julia: A fresh approach to numerical computing, SIAM Review, 59, 65-98, doi: 10.1137/141000671, 2017.

Crameri, F., Schmeling, H., Golabek, G.J., Duretz, T., Orendt, R., Buiter, S.J.H., May, D.A., Kaus, B.J.P., Gerya, T.V., Tackley, P.J.: A comparison of numerical surface topography calculations in geodynamic modelling: an evaluation of the 'sticky air' method. Geophysical Journal International 189, 38-54, doi: 10.1111/j.1365-246X.2012.05388.x, 2012.

Davaille, A.: Simultaneous generation of hotspots and superswells by convection in a heterogeneous planetary mantle. Nature 402, 756-760, doi:10.1038/45461, 1999.

- Deschamps, F., Kaminski, E., Tackley, P.J.: A deep mantle origin for the primitive signature of ocean island basalt. Nature Geosci. 4, 879-882, doi:10.1038/ngeo1295, 2011.
- Duretz, T., May, D. A., Gerya, T. V. and Tackley, P. J.: Discretisation errors and free surface stabilization in the finite difference and marker-in-cell method in geodynamic applications: A numerical study, Geochem. Geophys. Geosyst.,
- 270 12(Q07004), doi:10.1029/2011GC003567, 2011.
 - Dziewonski, A.M., Anderson, D.L.: Preliminary reference Earth model. Phys. Earth Planet. Inter. 25, 297-356, doi:10.1016/0031-9201(81)90046-7, 1981.
 - Gassmöller, R., Dannberg, J., Bangerth, W., Heister, T., and Myhill, R.: On formulations of compressible mantle convection, Geophys. J. Int., 221(2), 1264-1280, doi:10.1093/gji/ggaa078, 2020.
- 275 Gerya, T.V. and Yuen, D.A.: Robust characteristics method for modelling multiphase visco-elasto-plastic thermomechanical problems, Physics of the Earth and Planetary Interiors, 163, 83-105, doi:10.1016/j.pepi.2007.04.015, 2007. Gurnis, M.: The effects of chemical density differences on convective mixing in the Earth's mantle, *J. Geophys. Res.*, 91, 1407-1419, doi:10.1029/JB091iB11p11407, 1986.
 - Harlow, F.H. and Welch, J.E.: Numerical calculation of time-dependent viscous incompressible flow of fluid with free surface, Phys. Fluids A, 8, 2182-2189, doi:10.1063/1.1761178, 1965.
 - Kameyama, M., Kageyama, A. and Sato, T.: Multigrid-based simulation code for mantle convection in spherical shell using yin-yang grid, Phys. Earth Planet. Int., 171, 19-32, doi:10.1016/j.pepi.2008.06.025, 2008.
 - Kaus, B. J. P., Mühlhaus, H. and May, D. A.: A stabilization algorithm for geodynamic numerical simulations with a free surface, Phys. Earth Planet. Int., 181(1-2), 12-20, doi:10.1016/j.pepi.2010.04.007, 2010.
- 285 Kaus, B. J. P., Popov, A. A., Baumann, T. S., Püsök, A. E., Bauville, A., Fernandez, N. and Collignon, M.: Forward and inverse modelling of lithospheric deformation on geological timescales, NIC Series, 48, ISBN 978-3-95806-109-5, pp. 299, http://hdl.handle.net/2128/9842, 2016.
 - King, S.D., Lee, C., van Keken, P.E., Leng, W., Zhong, S., Tan, E., Tosi, N., Kameyama, M.C.: A community benchmark for 2-D Cartesian compressible convection in the Earth's mantle. Geophysical Journal International 180, 73-87,
- 290 doi:10.1111/j.1365-246X.2009.04413.x, 2010.
 - Kramer, S.C., Wilson, C.R., Davies, D.R.: An implicit free surface algorithm for geodynamical simulations. Physics of the Earth and Planetary Interiors 194–195, 25–37. https://doi.org/10.1016/j.pepi.2012.01.001, 2012.
 - Lin, J., Gerya, T.V., Tackley, P.J., Yuen, D.A., Golabek, G.J.: Numerical modeling of protocore destabilization during planetary accretion: Feedbacks from non-Newtonian rheology and energy dissipation, Icarus 213, 24-42, doi:10.1016/j.icarus.2009.06.035, 2011.
 - Nakagawa, T., Tackley, P.J.: Influence of plate tectonic mode on the coupled thermochemical evolution of Earth's mantle and core. Geochem., Geophys., Geosys. 16, 3400-3413, doi: 10.1002/2015gc005996, 2015.
 - Ogawa, M., Schubert, G. and Zebib, A.: Numerical simulations of 3-dimensional thermal convection in a fluid with strongly temperature-dependent viscosity, J. Fluid Mech., 233, 299-328, doi:10.1017/S0022112091000496, 1991.

- 300 Ogawa, M.: Numerical models of magmatism in convecting mantle with temperature-dependent viscosity and their implications for Venus and Earth, J. Geophys. Res. 105, 6997-7012, doi:10.1029/1999JE001162, 2000.
 - Patankar, S.V.: Numerical Heat Transfer and Fluid Flow, CRC Press, doi:10.1201/9781482234213, 1980.
- Popov, A.A., Sobolev, S.V.: SLIM3D: A tool for three-dimensional thermomechanical modeling of lithospheric deformation with elasto-visco-plastic rheology. Physics of the Earth and Planetary Interiors 171, 55–75, https://doi.org/10.1016/j.pepi.2008.03.007, 2008.
 - Rose, I., Buffett, B., Heister, T.: Stability and accuracy of free surface time integration in viscous flows. Physics of the Earth and Planetary Interiors 262, 90–100, https://doi.org/10.1016/j.pepi.2016.11.007, 2017.
 - Samuel, H., Tackley, P.J.: Dynamics of core formation and equilibrium by negative diapirism, Geochem. Geophys. Geosyst. 9, doi:10.1029/2007GC001896, 2008.
- 310 Schubert, G., Turcotte, D.L., Olson, P.: Mantle Convection in the Earth and Planets, Cambridge University Press, doi:10.1017/CBO9780511612879, 2001.
 - Tackley, P.J.: Effects of strongly temperature-dependent viscosity on time-dependent, 3-dimensional models of mantle convection, Geophys. Res. Lett., 20, 2187-2190, doi:10.1029/93GL02317, 1993.
 - Tackley, P.J.: Effects of strongly variable viscosity on three-dimensional compressible convection in planetary mantles. J.
- 315 Geophys. Res. 101, doi:3311-3332. doi.org/10.1029/95JB03211, 1996.

convection simulations" (1.0), Zenodo, doi:10.5281/zenodo.15115817.

- Tackley, P.J.: Three-dimensional simulations of mantle convection with a thermochemical CMB boundary layer: D"?, in: Gurnis, M., Wysession, M.E., Knittle, E., Buffett, B.A. (Eds.), The Core-Mantle Boundary Region, American Geophysical Union, pp. 231-253, doi: 10.1029/GD028, 1998.
- Tackley, P.J.: Modelling compressible mantle convection with large viscosity contrasts in a three-dimensional spherical shell
- 20 using the yin-yang grid. Phys. Earth Planet. Int., doi:10.1016/j.pepi.2008.1008.1005, 2008.
 Tackley P.J., ETH Zurich: Software for manuscript "On stabilisation of compositional density jumps in compressible mantle
 - Trompert, R.A. and Hansen, U.: The application of a finite-volume multigrid method to 3-dimensional flow problems in a highly viscous fluid with a variable viscosity, Geophys. Astrophys. Fluid Dyn., 83, 261-291,
- 325 doi:10.1080/03091929608208968, 1996.